Supplementary information

1. Solvent extraction experiments

Table S1. Distribution ratios of rare earth elements during extraction with ligands **L1-L3**. Composition of the aqueous phase: total concentration of rare earth elements 0.001 mol/L, 3 mol/L nitric acid. Composition of the organic phase: 0.1 mol/L **L1-L3** in F-3

D	La	Ce	Pr	Nd	Sm	Eu	Gd	Tb	Dy	Ho	Er	Tm	Yb	Lu
L1	0,04	0,03	0,01	0,01	0,01	0,01	0,01	<0,01	0,01	<0,01	<0,01	<0,01	0,01	<0,01
L2	0,05	0,03	0,02	0,02	0,01	0,01	0,01	0,01	0,01	0,01	0,01	<0,01	0,02	0,01
L3	0,02	0,02	0,01	0,01	0,02	0,03	0,02	0,01	0,02	0,01	0,01	0,01	0,02	0,02

Table S2. Conversion of **L1-3** ligands to the nitrate form upon contact with 3 mol/L nitric acid. Organic phase: 0.1 mol/L **L1-3** in meta-nitrobenzotrifluoride. Aqueous phase: 3 mol/L HNO_3.

	$C(Br^-)$, aqueous phase, mol/L	$C(Br^-)$, initial, mol/L	Conversion, %
L1	0.016	0.2	8.0
L2	0.015	0.2	7.3
L3	0.010	0.2	5.2

Table S3. Distribution ratios of thorium(IV) depending on the concentration of nitric acid. Organic phase: 0.1 mol/l **L1-3** or **L1N-3N** in F-3. Aqueous phase: $5\cdot10^{-4}$ mol/L thorium(IV) nitrate in 1-6 mol/L nitric acid.

$C(HNO_3)$, mol/L	1	2	3	4	5	6
L1	9.0	8.6	11.1	12.4	8.7	10.1
L2	13.1	11.8	18.2	17.6	14.5	16.5
L3	191.7	45.7	29.6	24.8	22.2	14.7
L1-N	21.3	30.9	28.1	25.6	26.7	22.4
L2-N	114.7	52.2	40.8	38.1	42.1	36.5
L3-N	208.6	44.0	48.9	52.2	50.3	35.1

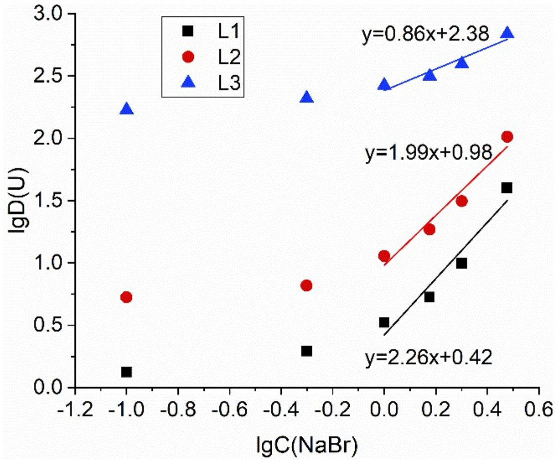

Figure S1. Dependence of the logarithm of the uranium(VI) distribution ratio on the logarithm of the sodium bromide concentration. Aqueous phase: $5\cdot10^{-4}$ uranyl nitrate, 0.05 mol/L nitric acid, sodium bromide concentration range from 0.1 to 3 mol/L. Organic phase: 0.1 mol/L **L1-L3** in F-3.

At bromide concentrations less than 1 mol/L, the distribution ratios increase slightly. The absence of a pronounced dependence in this case may indicate that additional bromide ions are not part of the extracted complex. At higher bromide concentrations distribution ratios begin to increase significantly, and for the graph of the lgD(U) dependence on the lgC(NaBr) concentration, the points are described by a straight line with a slope of about 2 for **L1** and **L2** and 1 for **L3**. Such slope values may indicate the extraction of uranium(VI) in the form of a bromide complex with a large excess of bromide ions in the system, i.e., the uranyl cation during extraction binds with two additional bromide ions in the case of **L1** and **L2** or with one bromide in the case of **L3**.

2. XANES

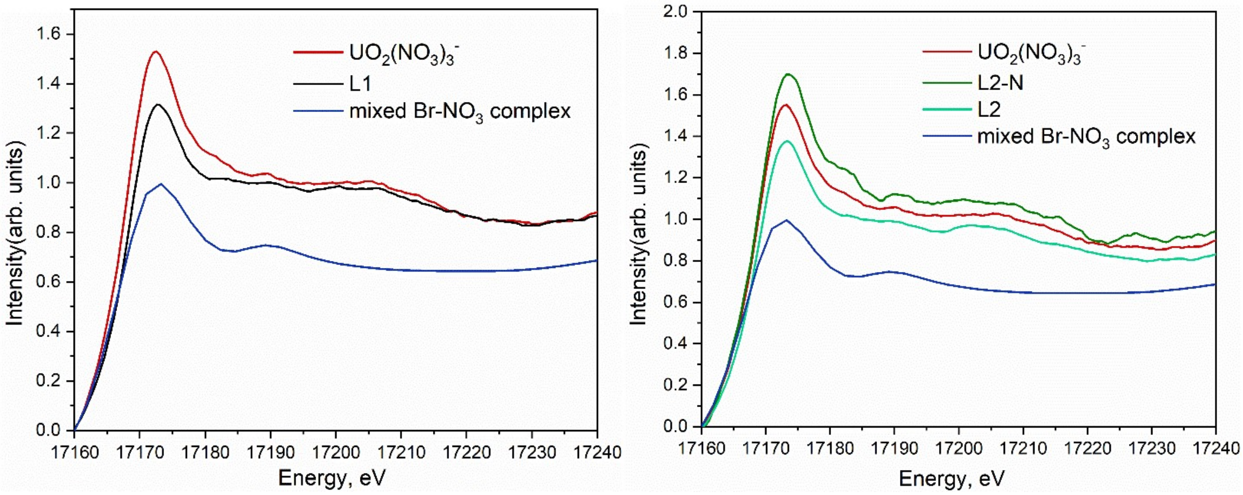

Figure S2. XANES spectra for 0.1 mol/L **L1** (left) and **L2**, **L2-N** (right) in F-3 after extraction of excess uranyl nitrate in 3 mol/L nitric acid in comparison with the reference spectra.

3. X-ray diffraction analysis

Table S4. Crystal data and structure refinement for crystals of **L1** with U(VI) and **L3** with U(VI).

Identification code	L1_U	L3_U
CCDC	2498070	2481655
Empirical formula	$C_{26}H_{58}N_4O_{14}P_2U$	$C_{28}H_{62}Br_{2.65}N_{1.34}O_{6.04}P_2U$
Formula weight	950.73	1026.31
Temperature/K	100	100
Crystal system	monoclinic	monoclinic
Space group	$P2_1/n$	$P2_1/c$
a/Å	12.5385(11)	17.1103(7)
b/Å	14.5329(10)	15.2774(6)

c/Å	20.9539(15)	16.2613(6)
α/°	90	90
β/°	91.168(3)	110.3210(10)
γ/°	90	90
Volume/Å^3	3817.4(5)	3986.2(3)
Z	4	4
ρ_{calc}g/cm^3	1.654	1.710
μ/mm^{-1}	4.400	6.849
F(000)	1904.0	2010
Crystal size/mm^3	0.33 × 0.31 × 0.2	0.28 × 0.25 × 0.05
Radiation	MoKα (λ = 0.71073)	MoKα (λ = 0.71073)
2Θ range for data collection/°	3.41 to 61.162	3.682 to 56.996
Reflections collected	49200	79960
Independent reflections	11617 [R_{int} = 0.0984, R_{sigma} = 0.0929]	10101 [R_{int} = 0.0864, R_{sigma} = 0.0630]
Data/restraints/parameters	11617/0/430	10101/43/427
Goodness-of-fit on F^2	1.019	1.027
Final R indexes [I>=2σ (I)]	R_1 = 0.0470, wR_2 = 0.0861	R_1 = 0.0388, wR_2 = 0.0799
Final R indexes [all data]	R_1 = 0.0780, wR_2 = 0.0986	R_1 = 0.0575, wR_2 = 0.0866
Largest diff. peak/hole / e Å^{-3}	0.93/-1.82	1.98/-2.28

4. Raman spectroscopy

In all spectra, except for the L+U in 1M HNO_3 system, all the peaks indicated in the main section are present, corresponding to the tri- and tetranitrate complexes of uranyl. The low intensity of all scattering lines in the L+U in 1M HNO_3 spectra is attributed to a lower concentration of dissolved species.

In the spectrum of the crystal with ligand 1, a shift of the scattering line in the 860 cm^{-1} region is observed, indicating a change in the uranium-oxygen bond coordination within the uranyl cation upon solid-phase formation compared to the solution. Furthermore, the spectrum of this crystal exhibits a most pronounced line corresponding to the uranyl tetranitrate complex, the presence of which was confirmed by SC-XRD.

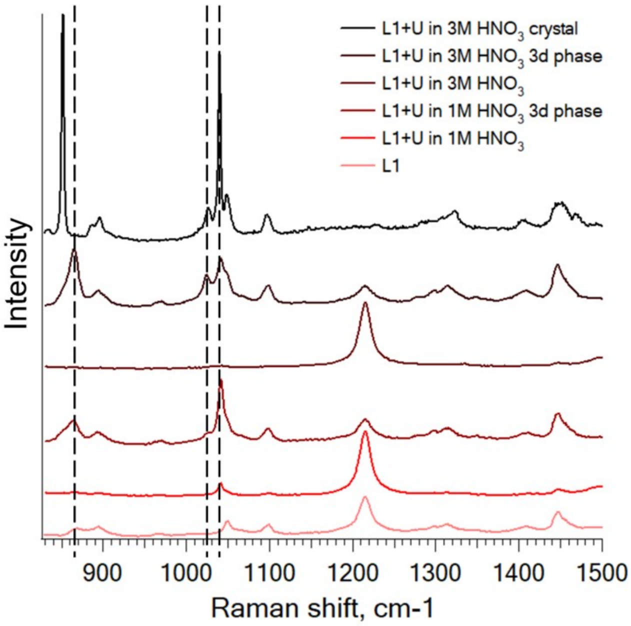

Figure S3. Raman spectra of pure ligand **L1** in chloroform and ligand saturated with uranyl nitrate in 1 or 3 mol/L nitric acid (**L**+U), as well as the uranium(VI) crystal with **L1**.

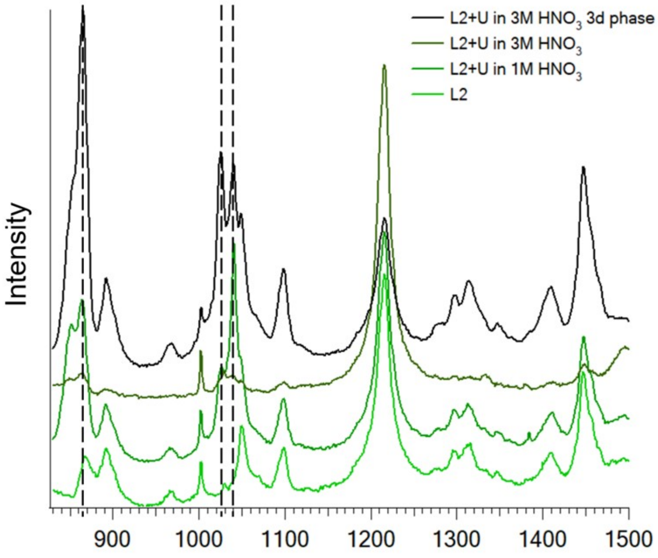

Figure S4 Raman spectra of pure ligand **L2** in chloroform and ligand saturated with uranyl nitrate in 1 or 3 mol/L nitric acid (**L**+U).

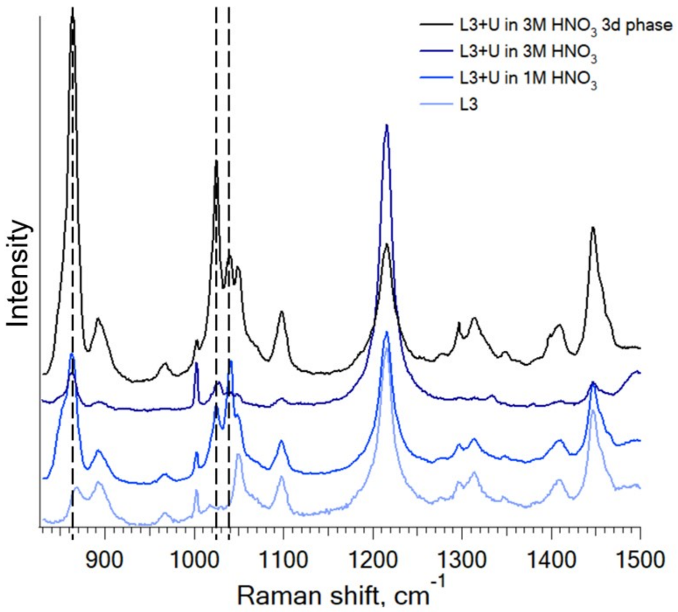

Figure S5 Raman spectra of pure ligand **L3** in chloroform and ligand saturated with uranyl nitrate in 1 or 3 mol/L nitric acid (**L**+U).

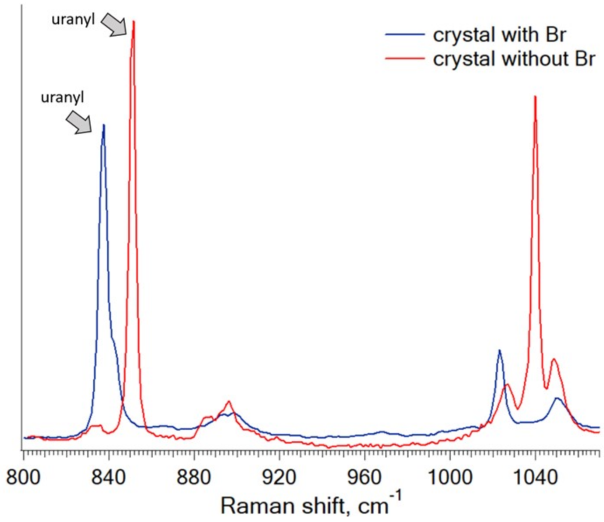

Figure S6. Raman spectra of crystals of uranyl complexes with **L1** (with Br) and **L3** (without Br).

In the spectrum of a crystal known to contain bromine, a shift of the uranyl band to the lower frequency region was observed compared to the crystal where only uranyl bonds with the nitrate ligand are present (851 and 837 cm^{-1}, respectively).

5. Infrared Spectroscopy

Infrared spectra were recorded for all the crystals obtained. The figure on the left shows data for crystals containing ligand **L1** and a uranyl tetranitrate complex, which were obtained from different solutions: by contacting a solution of the ligand in F-3 with uranyl nitrate in 3 or 1 mol/L nitric acid. In the latter case, the crystal formed from two different organic phases. The figure on the right shows the spectrum of a crystal of a mixed uranyl complex with ligand **L3**.

Peaks 1025, 1290, 1478 (crystals with **L1**), 1515 (crystal with mixed bromide-nitrate complex of uranyl and **L3**) cm^{-1} are attributed to nitrate [1,2], the peak at 920 cm^{-1} corresponds to the uranyl cation [2], and in the region of 2800-3000 P-H stretching bands may be overlapped with CH2 stretching vibrational bands [3].

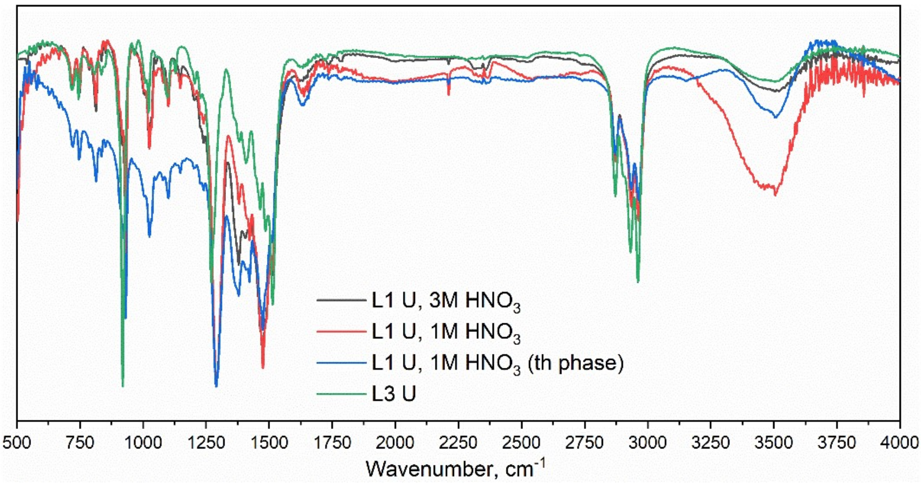

Figure S7. Infrared spectra of crystals of uranyl complexes with **L1** and **L3**.

6. Electrospray Ionization-Mass Spectrometry

The method shows the presence of the uranyl trinitrate complex in the organic phase after extraction.

Positive

*0.1 mol/L **L1-L3** in F-3/1 mol/L $UO_2(NO_3)_2$ in 3 mol/L HNO_3*

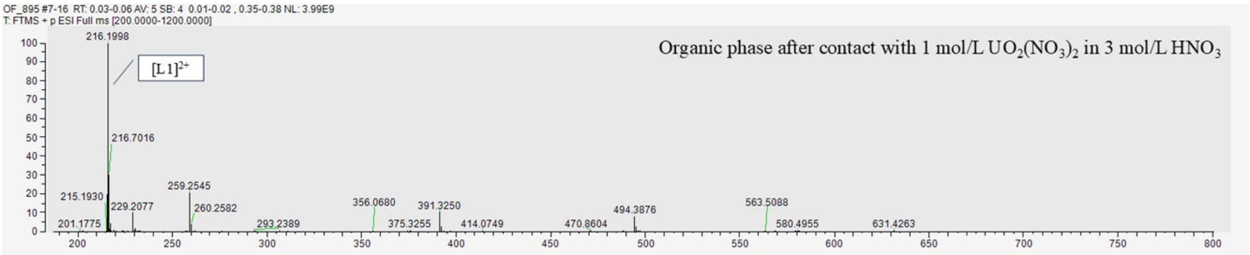

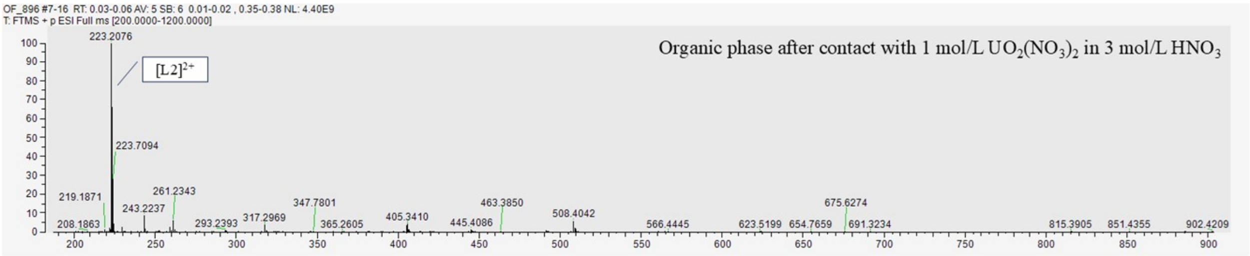

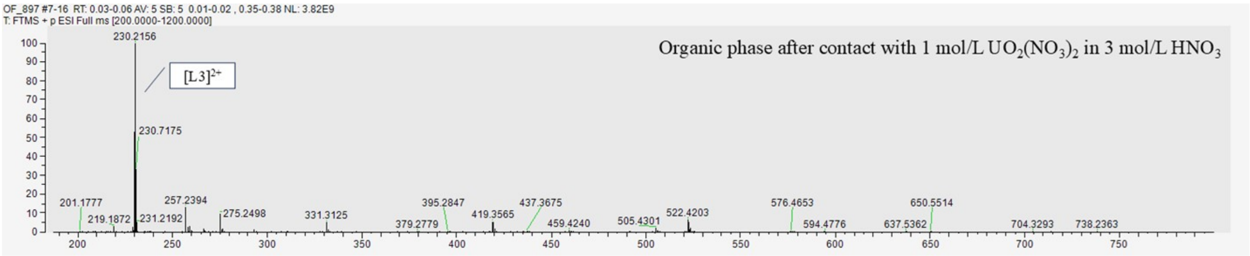

*0.1 mol/L **L1-L3** in F-3/1 mol/L $UO_2(NO_3)_2$ in 1 mol/L HNO_3*

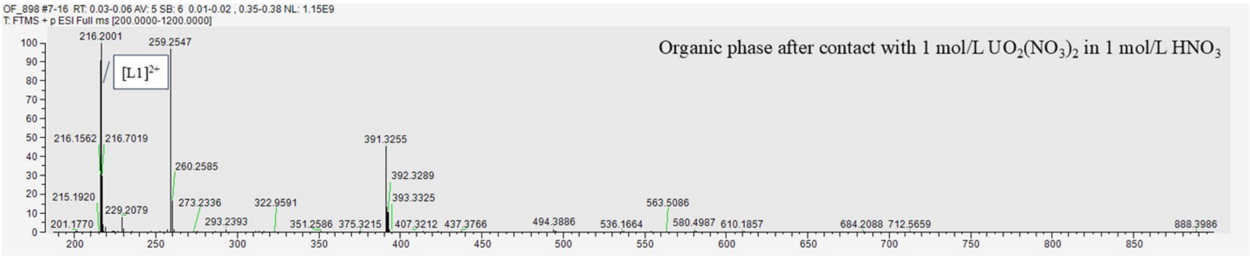

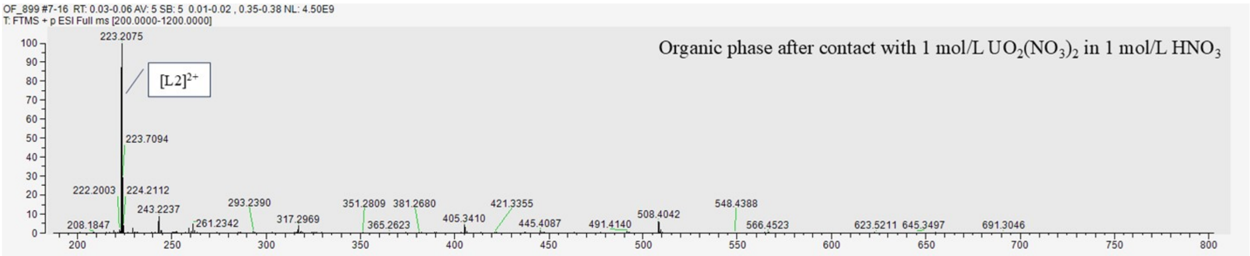

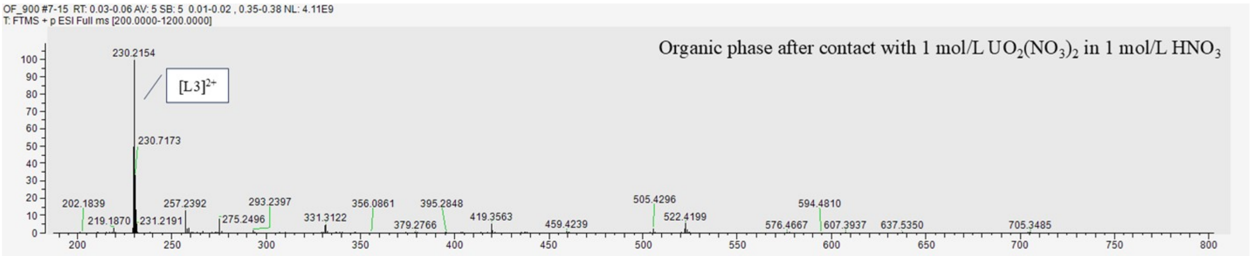

*0.1 mol/L **L1-L3** in F-3/0.1 mol/L $UO_2(NO_3)_2$ in 1 mol/L NaBr and 0.1 mol/L HNO_3*

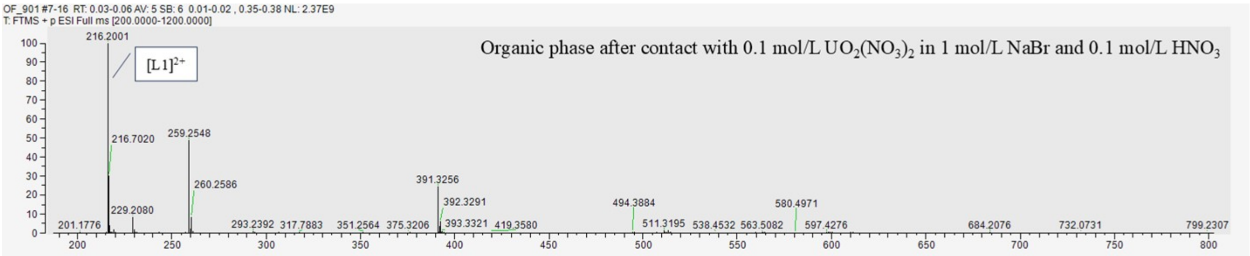

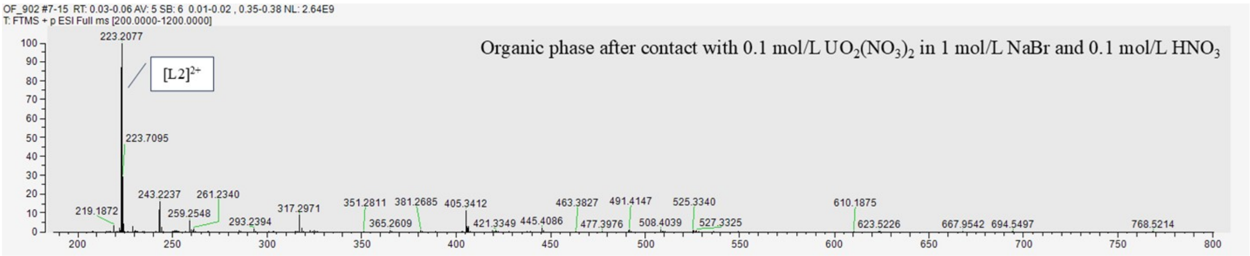

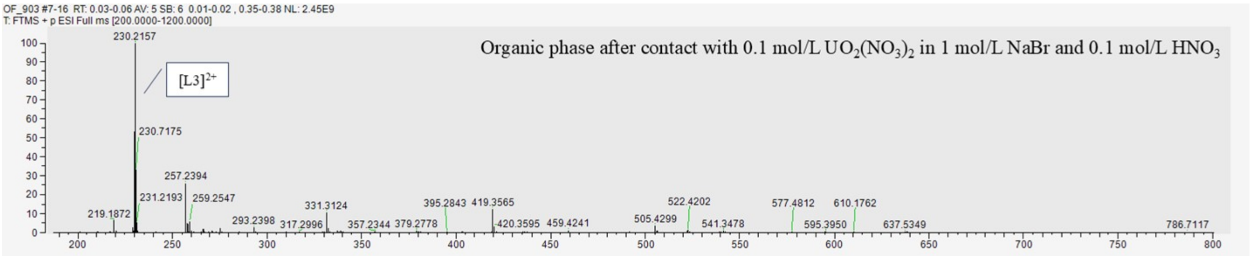

<u>Negative</u>

*0.1 mol/L **L1-L3** in F-3/1 mol/L $UO_2(NO_3)_2$ in 3 mol/L HNO_3*

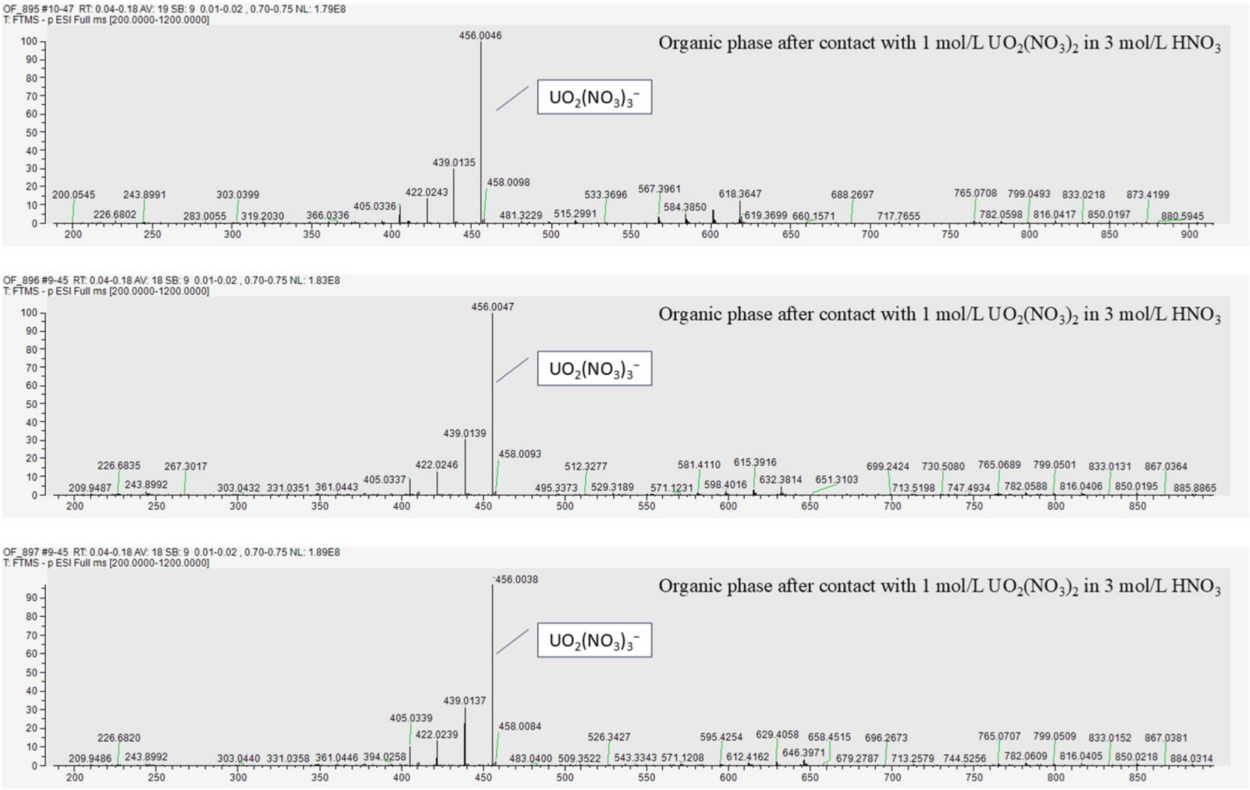

*0.1 mol/L **L1-L3** in F-3/1 mol/L $UO_2(NO_3)_2$ in 1 mol/L HNO_3*

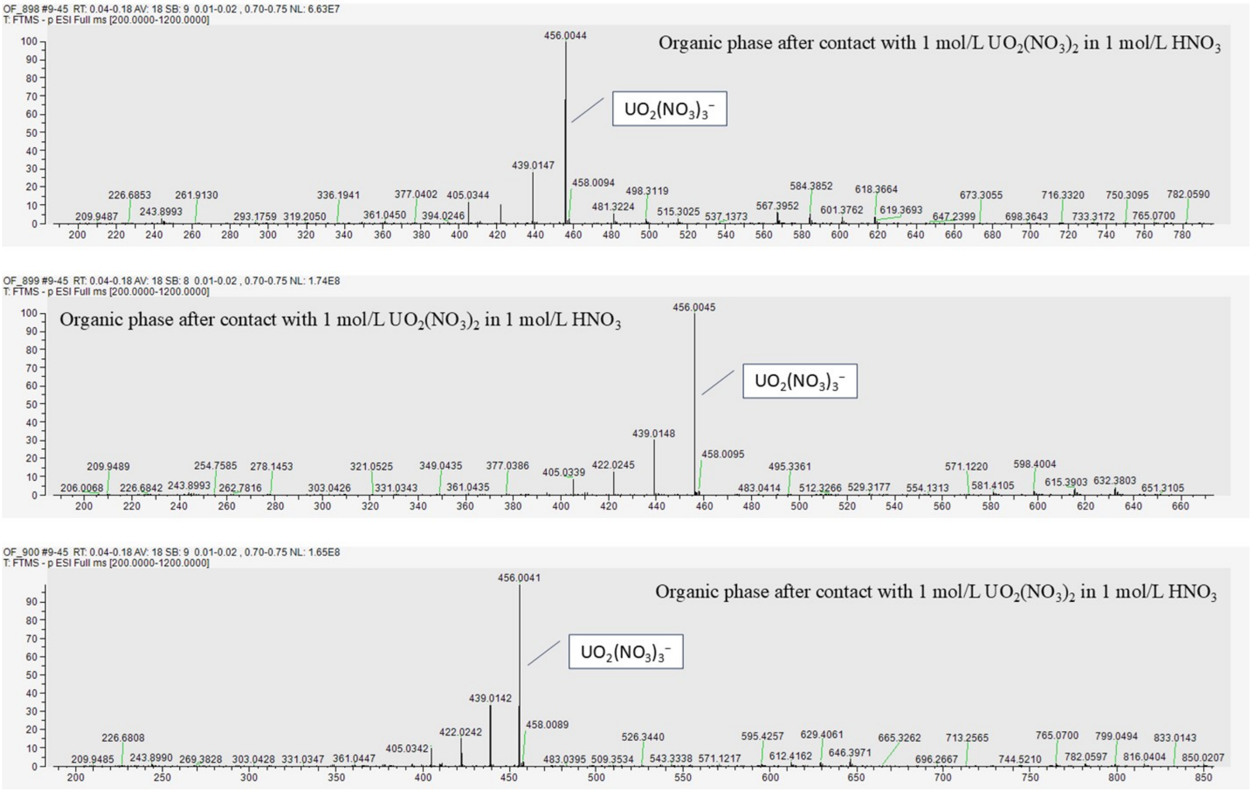

*0.1 mol/L **L1-L3** in F-3/0.1 mol/L $UO_2(NO_3)_2$ in 1 mol/L NaBr and 0.1 mol/L HNO_3*

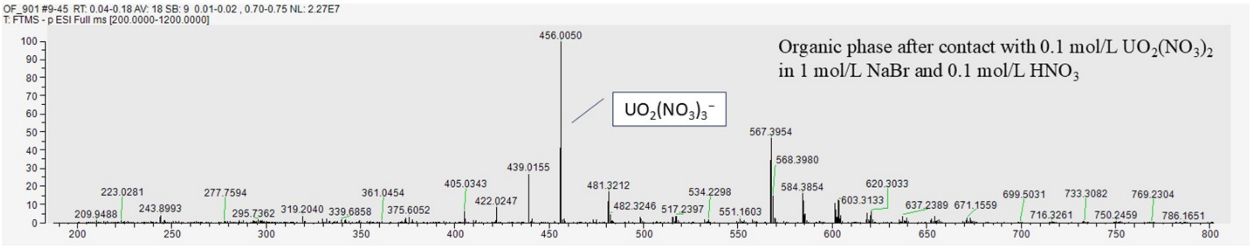

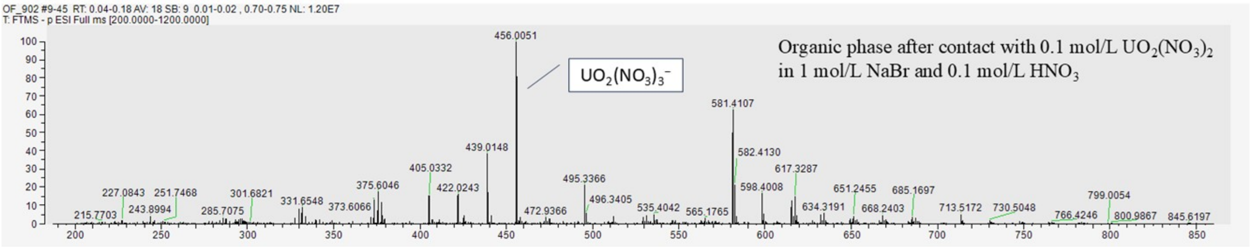

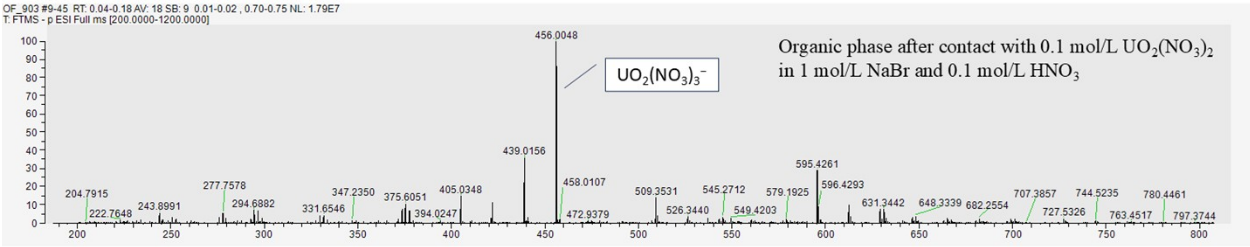

References

1. Mihaylov M.Y. et al. Infrared spectra of surface nitrates : Revision of the current opinions based on the case study of ceria // J. Catal. Elsevier Inc., 2021. Vol. 394. P. 245–258.

2. Volod'ko L. V., Komyak A. I. P.M.R. THE IR SPECTRA IN POLARIZED LIGHT STRUCTURE OF CRYSTALS OF URANYL TRI- AND TETRANITRATES // J. Appl. Spectrosc. 1969. Vol. 11, № 6. P. 1520–1525.

3. Luo J., Conrad O. V.I.F.J. Physicochemical properties of phosphonium-based and ammonium-based protic ionic liquids // J. Mater. Chem. 2012. Vol. 22, № 38. P. 20574–20579.